

Dual-Orthogonal Polarized Antenna for UWB-IR Technology

Grzegorz Adamiuk, *Student Member, IEEE*, Stefan Beer, Werner Wiesbeck, *Fellow, IEEE*, and Thomas Zwick, *Senior Member, IEEE*

Abstract—This paper presents a design of a dual-orthogonal, linear polarized antenna for the IR-UWB technology in the frequency range from 3.1 GHz to 10.6 GHz. The antenna is compact with dimensions of 40x40 mm of the radiation plane, which is orthogonal to the radiation direction. Both, the antenna and the feeding network are realized in planar technology. The radiation principle and the computed design are verified by a prototype. The input impedance matching is better than -6 dB. The measured results show a mean gain in co-polarization close to 4 dBi. The cross polarizations suppression w.r.t. the co-polarization is better than 20 dB. Due to its features the antenna is suited for polarimetric ultra wideband radar and ultra wideband MIMO applications.

Index Terms—Antennas, UWB, polarization diversity, differential feed.

I. INTRODUCTION

THE UWB mask defined by the FCC [1] allows the licence free usage of the spectrum between 3.1 GHz and 10.6 GHz with the maximal power spectral density of 41.3 dBm/MHz. A free of charge usage of the bandwidth opens many possibilities especially in localization and radar techniques, where the accuracy/ranging resolution is directly proportional to the bandwidth. One possibility of realizing signals that cover the mentioned bandwidth are very short pulses, which meet the spectrum regulation requirements. However the bandwidth of 7.5 GHz implies a big challenge for the antenna design, which is an essential part of any wireless system. The requirements regarding the antenna for the mentioned application include a linear phase response for the non-distorting impulse radiation.

In the literature several types of antennas designed for the mentioned frequency range can be found. Most of them are biconical structures [2], traveling wave radiators [3] or even combination of both [4]. However almost all solutions proposed in the literature offer only a single polarization operation, while many applications such as e.g. the UWB radar can benefit from dual-polarization [5]. The requirement on such an antenna is, apart from the above mentioned, a common radiation phase center for both polarizations. This allows for the identical radiation conditions for both polarizations. The requirement for the common phase center reduces the number of possible solutions for such an antenna. These are e.g. quad-ridged horn antennas [6] and derivatives [7], or dual-polarized dielectric rod radiators [8]. These antennas generally lead to

a bulky solution and are hardly integrable into any devices. For this reason a planar solution has been investigated. The problem to solve is how to design a surface that maintains the following features: radiation over a very large bandwidth with two orthogonal, linear polarizations, same phase center of radiation for both polarizations, relatively constant radiation pattern over the frequency range and radiation perpendicular to the surface. This publication introduces a solution for the antenna meeting the mentioned specifications.

In the following section the antenna geometry is introduced and the benefits of the proposed structure are described. Next the prototype is shown and the simulation and measurement results are presented and discussed.

II. ANTENNA PRINCIPLE

The proposed antenna for each polarization consists of two elliptically shaped dipoles surrounded by a ground plane as shown in Fig. 1(b). The dipoles for the orthogonal polarizations are orthogonal to each other and are in contrast to usual dipoles not center fed. The feeding is placed on the outer side between the ground plane and the single ellipse. This allows a spacial separation of the feedings for both polarizations. Such an arrangements results in four monopoles. The two inline monopoles are fed simultaneously in order to radiate a single linear polarization. The polarization direction is marked by the orientation of the excited ellipses. The orientation of the electric field at the feeding point has to be co-polarized as shown in Fig. 1(b) by arrows. However, considering the orientation of the electric field vectors relatively to the ground plane, the two monopoles are fed differentially. The idea of the differential feeding and its application for wideband antennas can be found in the literature [9], [10]. However the proposed solutions did not allow for the application of the antennas in IR-UWB systems. The design proposed here bases on a principle introduced by the authors in [11].

Each of the monopoles itself is an ultra wideband antenna. Due to the circular ground plane around the radiator, the radiation of the monopole is not torus like, but bidirectional and perpendicular to the antenna surface. The symmetrical arrangement of two monopoles in the circle for the single, linear polarization helps to keep the current distribution in the radiation zone symmetrically w.r.t. the center of the antenna. Such current distribution results in a symmetrical radiation pattern, which is optimized to be very stable over the frequency range. Due to the symmetry of the current distribution, the phase center of radiation of a single polarization is exactly

The Authors are with the Institut fuer Hochfrequenztechnik und Elektronik, Universitaet Karlsruhe (TH), Kaiserstr. 12, 76131, Karlsruhe, Germany, email:grzegorz.adamiuk@ihe.uka.de

between the two monopoles in the center of the structure. Its position is independent of the frequency. This is a big advantage in impulse radiating UWB antennas, since it does not distort the radiating pulse [14]. Noticeable is that for the orthogonal polarization the phase center of radiation is exactly at the same place. This ensures identical radiation conditions for both polarizations. This is advantageous in e.g. imaging or radar.

Another advantage of the antenna is a high decoupling between the pairs of ports for orthogonal polarizations. Since the orientation of the electric field vectors for orthogonal polarizations is cross polarized, the energy fed into one pair of the ports does not couple to the second pair. This avoids firstly the undesired coupling of the energy to the other ports. Secondly it assures a good polarization decoupling in the far-field since the currents are not re-radiated by the orthogonal monopoles.

The dimensions of the whole structure are 40 mm x 40 mm. The opening in the ground plane has a diameter of 31.6 mm. It means that the half of the circumference is approx. 50 mm. This corresponds to half a wavelength in free space at 3 GHz, which corresponds to the lower limit of the targeted frequency range. An optimization procedure resulted in a very broadband impedance matching that covers the FCC UWB frequency range. During the optimization the far-field properties of the antenna were also considered. The relative orientation of the dipoles to each other and their shape produces different current distributions, which result in the deformation of the radiation pattern. The structure was optimized in order to find a compromise between a good matching and appropriate radiation pattern. In the design the outer form of the ground plane was formed to a square, but it can be shaped also to a ring with a minimum width of 5 mm.

The hardware realization of the antenna requires a number of design and optimizations steps, which were mainly conducted with the help of a commercial simulation software [12]. The single input for each polarization has to be divided into two wideband baluns, which feed the two monopoles. For this purpose the input microstrip line is divided into two lines by a 3 dB power divider. Next the ground plane of each of the microstrip lines is tapered in order to achieve a symmetrical field distribution (see Fig. 2). An important optimization criterion is the equality of amplitude and phase at both outputs for the single monopoles. The output of the wideband baluns has to be matched to the input impedance of the monopoles in order to avoid multiple reflections and

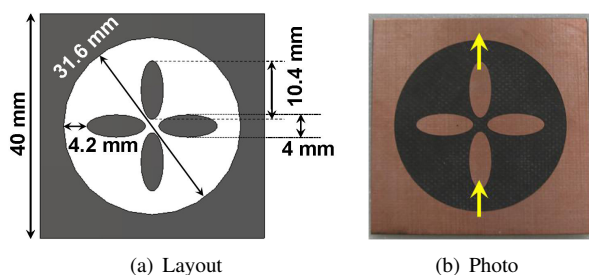


Fig. 1. The proposed antenna

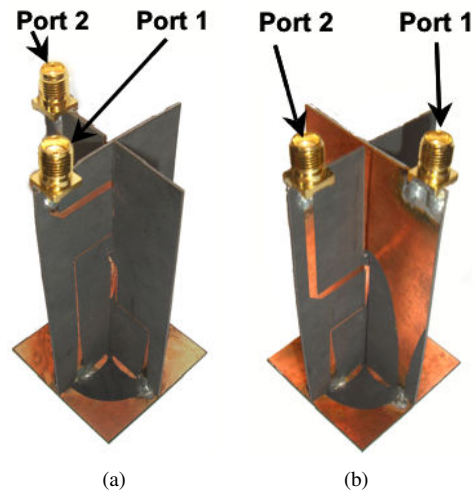


Fig. 2. Prototype with the feeding networks for both polarizations in two different views (a) and b)

thus ringing [14]. In the next step the feeding lines for each polarization are separated from each other. This is realized by a longitudinal disalignment of the power dividers and respective adjustment of the strip lines. Such an arrangement allows a physical crossing of both substrates without any intersection of the high-frequency waveguides. The principle can be seen in Fig. 2.

The antenna radiates bidirectionally (forward and backward). Thus the feeding networks are directly illuminated and the electromagnetic wave is scattered and reflected from the baluns. It deforms the radiation pattern and produces contributions in both, co- and cross-polarizations. Since an implementation of a reflector in the considered design would degrade the bandwidth of the antenna, the radiation in the backward direction is absorbed. It results in an a priori loss of 3 dB. However a directional and purely polarized radiation is achieved, which is shown in the next section.

For the proper interpretation of the results the antenna is placed in a coordinate system in Fig. 3, where also the respective ports are marked.

III. RESULTS AND DISCUSSION

In Fig. 4 the measured and simulated S-parameters of the antenna are shown. Since UWB technique deals with very low power the requirement on the input impedance matching can be relaxed to less than -10 dB. This simplifies the optimization process of the relatively complicated structure. The so defined requirements on the parameters are well fulfilled for both

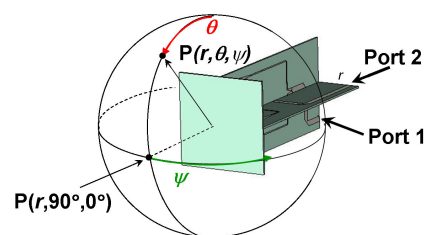


Fig. 3. Definition of the angles relatively to the antenna

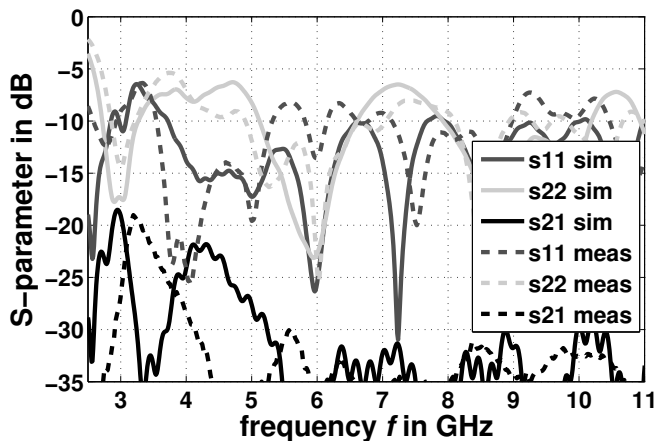


Fig. 4. Simulated and measured S-parameters of the antenna.

ports in the desired bandwidth. As expected the decoupling between the ports is very high and above approx. 25 dB in almost the whole frequency range. The simulation predicted the general behavior of the antenna well, which is confirmed by the similarity of simulated and measured curves.

The antenna's radiation properties are measured in an anechoic chamber. The result of the gain measurement for port 2 in the H -plane (see Fig. 2 and Fig. 3) for co-polarization is shown in Fig. 5. Since the backward radiation is fully absorbed, a directive radiation can be observed. The gain in the main beam direction ($\theta = 90^\circ, \psi = 0^\circ$) rises from approx. 2 dBi at the lower, to over 5 dBi at the higher frequencies. The shape of the beam remains relatively constant over the whole designated frequency range. The measured radiation pattern in the E -plane shows very similar shape and is not specifically shown. The measurement at port 1 showed the similarity of the respective planes at both ports and is also not specifically shown. Some differences in the magnitudes at both polarizations occur due to the differences in the impedance matching at both ports due to the slightly different feeding networks.

In pulse mode operation the signal is radiated over the whole bandwidth simultaneously. For this reason one single value characterizing the power radiated in the specified direction is desirable. Such value is e.g. the mean gain G_m . It is defined as an arithmetic mean of all gain values G in the regarded frequency range. The formula for the calculation of the mean gain G_m from the discrete, frequency dependent gain values is:

$$G_m = \frac{1}{N} \sum_{n=1}^N G(f_n, \theta, \psi), \quad (1)$$

where G is the gain of the antenna, N is the number of the measured frequency points and ψ, θ are the azimuth and elevation angles, respectively.

The so calculated gain in the frequency range from 3.1 GHz to 10.6 GHz is shown in Fig. 6 for port 1 and in Fig. 7 for port 2, for E - and H -plane. During the measurements the other input of the antenna is terminated with 50Ω . It can be

noticed that the characteristics are nearly symmetrical to the main beam direction. A slightly smaller mean gain (approx. 0.5 dBi) at port 1 in the main beam direction can be observed due to previously mentioned impedance matching differences. As noted before both planes exhibit very similar radiation properties, since the apertures of the antennas have the same dimensions.

For the evaluation of dual-polarized antennas the cross polarized characteristics are vital. These are shown in the Fig. 6 and Fig. 7 as well. The mean gain for the cross polarized components in the main beam direction is more than 20 dB lower than the co-polarized gain.

In order to evaluate the impulse radiating properties of the antenna another quantity is needed that includes also the phase behavior of the antenna radiation. A very intuitive parameter that describes also the distortion properties of the radiated pulse is the impulse response $h(t, \theta, \psi)$. This can be calculated from the transfer function of the antenna $H(f, \theta, \psi)$, which can be obtained from the complex frequency domain measurement and proper calibration of the system. The calculated complex transfer function $H(f, \theta, \psi)$ is transformed into the time domain by Fourier transform

$$h(t, \theta, \psi) = \mathcal{F} \{ H(f, \theta, \psi) \}. \quad (2)$$

The exact description of the procedure can be found in [13], [14]. The antenna radiates properly an impulse when the amplitude of the impulse response is high, the duration of it is short and when there is no ringing after the main pulse. For an exact description of the parameters characterizing the impulse response of an antenna it is referred to the [13], [14].

The impulse response of the antenna in the H -plane for co-polarization can be seen in Fig. 8. The impulse response is very short with approx. 130 ps for the main beam direction. This short impulse response implies a high concentration of the energy in the time domain. The peak value of $|h(t)|$ is relatively high for $\theta = 90^\circ$ and $\psi = 0^\circ$ and equals approx. 0.23 m/Vs. After the main peak a weak ringing can be observed, which

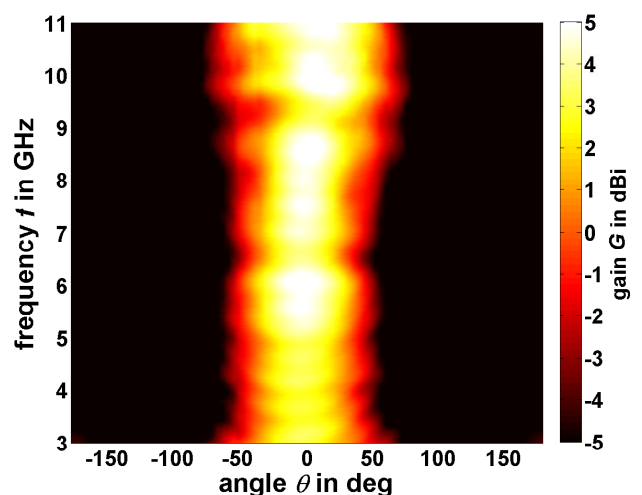


Fig. 5. Measured gain $G(f, \theta, \psi = 90^\circ)$ of the antenna fed at port 2 in the H -plane for Co-polarization.

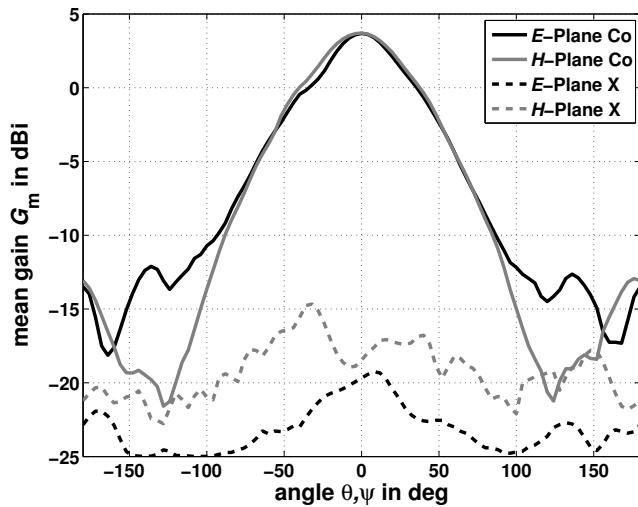


Fig. 6. Measured mean gain $G_m(\theta, \psi)$ of the antenna fed at port 1 in the E - and H -plane for Co- and X-polarization.

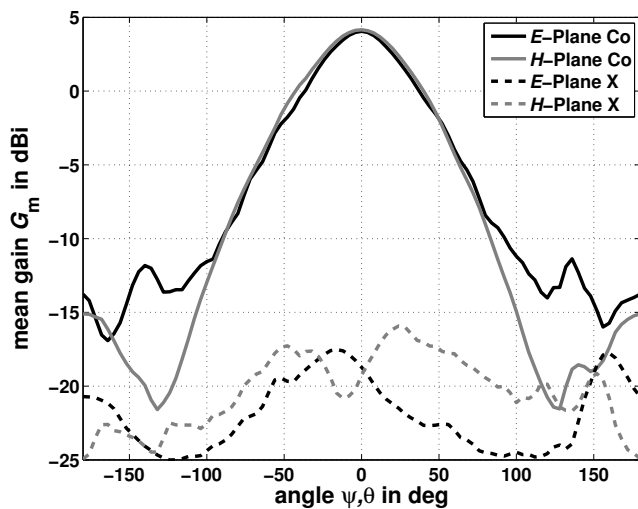


Fig. 7. Measured mean gain $G_m(\theta, \psi)$ of the antenna fed at port 2 in the E - and H -plane for Co- and X-polarization.

causes small oscillations of the radiated impulse after the main pulse. The ringing results mainly from reflections from the feeding network.

IV. CONCLUSIONS

In this paper a solution for the realization of a planar, dual-polarized UWB antenna is presented. The antenna covers the frequency range between 3.1 GHz and 10.6 GHz. In this frequency range the radiation pattern of the antenna remains stable and directive. The properties of the antenna have been verified by measurements of the prototype. Both, E - and H -plane show similar radiation properties. The principle of the antenna yields very good polarization decoupling in the far-field and good decoupling between the ports over the whole bandwidth. Both polarizations have the same radiation phase center, which is stable versus frequency. Based on the impulse

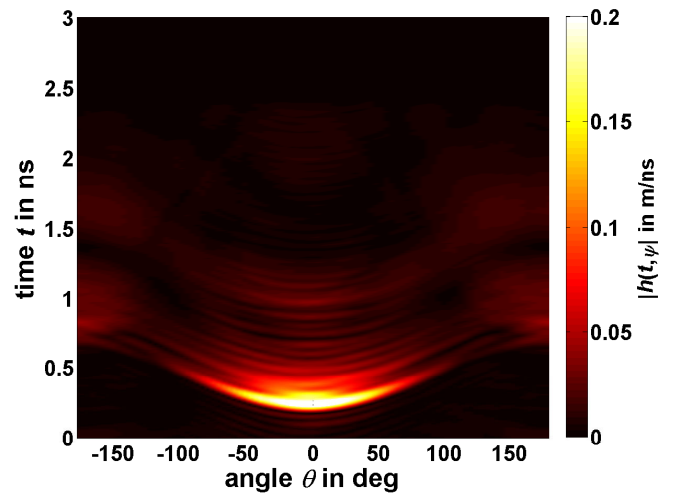


Fig. 8. Measured impulse response $h(t, \theta, \psi = 90^\circ)$ of the antenna fed at port 2 in the H -Plane for Co-polarization.

response it has been shown that the antenna is suitable for impulse based UWB systems.

REFERENCES

- [1] Federal Communications Commission (FCC), "Revision of Part 15 of the Commissions Rules Regarding UltraWideband Transmission Systems", First Report and Order, ET Docket 98-153, FCC 02-48; Adopted: February 2002; Released: April 2002
- [2] C. A. Balanis, "Antenna Theory: Analysis and Design", Wiley & Sons, New York, NY, USA, 1996
- [3] A. Elsherbini, Z. Cemin, L. Song, M. Kuhn, A. Kamel, A.E. Fathy, H. Elhennawy, "UWB antipodal vivaldi antennas with protruded dielectric rods for higher gain, symmetric patterns and minimal phase center variations", IEEE Antennas and Propagation International Symposium, pp. 1973 - 1976, Honolulu, 9-15 June 2007
- [4] M.D. Blech, T.F. Eibert, "A Dipole Excited Ultrawideband Dielectric Rod Antenna With Reflector", IEEE Transactions on Antennas and Propagation, vol. 55, issue 7, pp. 1948 - 1954, July 2007
- [5] R. Zetik, J. Sachs, R. Thomae, "UWB Short Range Radar Sensing" IEEE Instrumentation and Measurement Magazine, vol. 10, pp. 39 - 45, April 2007
- [6] ETS-Lindgren, www.ets-lindgren.com
- [7] I.A. Osaretin, A. Torres, C. Chen, "A Novel Compact Dual-Linear Polarized UWB Antenna for VHF/UHF Applications", IEEE Antennas and Wireless Propagation Letters, Accepted for future publication, available in IEEExplore
- [8] J.-Y. Chung, C. Chen, "Two-Layer Dielectric Rod Antenna", IEEE Transactions on Antennas and Propagation, vol. 56, issue 6, pp. 1541 - 1547, June 2008
- [9] R. C. Paryani, P. F. Wahid, N. Behdad, "A wide-band, dual-polarized, differentially-fed cavity-backed slot antenna", 2008 URSI General Assembly, August 7-16 2008, Chicago
- [10] S.-Y. Suh, A.E. Waltho, V.K. Nair, W.L. Stutzman, W.A. Davis, "Evolution of broadband antennas from monopole disc to dual-polarized antenna", IEEE Antennas and Propagation Society International Symposium 2006, pp. 1631 - 1634, Albuquerque, New Mexico, 9-14 July 2006
- [11] G. Adamiuk, W. Wiesbeck, T. Zwick, "Differential Feeding as a Concept for the Realization of Broadband Dual-Polarized Antennas with Very High Polarization Purity", IEEE Antennas and Propagation Society International Symposium 2009, Charleston, 1-5 June 2009
- [12] CST Microwave Studio, www.cst.com
- [13] E. G. Farr, C. E. Baum, "Extending the definitions of antenna gain and radiation pattern into the time domain", Sensor and Simulation Notes, note 350, Directed Energy Directorate, Air Force Research Laboratory, Kirtland, NM, USA, 1992
- [14] W. Soergel, W. Wiesbeck, "Influence of the Antennas on the Ultra Wideband Transmission", EURASIP Journal on Applied Signal Processing, special issue UWB - State of the Art, pp. 296 - 305, March 2005